



# Laser-controlled production of Rydberg positronium via charge exchange collisions

A. Speck<sup>a</sup>, C.H. Storry<sup>a</sup>, E.A. Hessels<sup>b</sup>, G. Gabrielse<sup>a</sup>

<sup>a</sup> Department of Physics, Harvard University, Cambridge, MA 02138, USA

<sup>b</sup> York University, Department of Physics and Astronomy, Toronto, ON M3J 1P3, Canada

Received 5 June 2004; received in revised form 19 July 2004; accepted 22 July 2004

Available online 29 July 2004

Editor: L. Rolandi

## Abstract

Lasers are used to choose the binding energies of highly excited positronium atoms ( $\text{Ps}^*$ ) created via charge exchange collisions. The lasers directly excite cesium (Cs) atoms to highly excited states ( $\text{Cs}^*$ ). These large  $\text{Cs}^*$  atoms have a large cross section for resonant charge exchange collisions with trapped positrons. Highly excited  $\text{Ps}^*$  is formed with a binding energy that is determined by the initial laser excitation. These  $\text{Ps}^*$  should have a large cross section for resonant charge exchange collisions with trapped antiprotons—suggesting a possible new way to produce cold antihydrogen.

© 2004 Published by Elsevier B.V.

The formation of a cold antihydrogen ( $\bar{\text{H}}$ ) atom, from an antiproton ( $\bar{\text{p}}$ ) and a positron ( $\text{e}^+$ ), requires the participation of a third body for energy and momentum to be conserved. To achieve the long term goal of forming cold  $\bar{\text{H}}$  for trapping and spectroscopy [1] several such formation mechanisms have been proposed [2–6]. For a charge exchange collision of a positronium (Ps) and a trapped antiproton,  $\text{Ps} + \bar{\text{p}} \rightarrow \bar{\text{H}} + \text{e}^-$  [2], the electron is the needed third body. The counterpart process in which a proton (p) is substituted for a  $\bar{\text{p}}$  has been used to produce hydrogen instead of  $\bar{\text{H}}$  [7]. However, the observed rate was slow and many fewer

$\bar{\text{p}}$  than p are available so no attempt has been made to form  $\bar{\text{H}}$  by this method. The cross section and rate for  $\bar{\text{H}}$  formation from collisions of  $\bar{\text{p}}$  with highly excited Rydberg Ps would be very much larger. Ps production by laser excitation was thus proposed [4] but never realized.

This Letter reports a demonstration of a promising alternative—producing Rydberg  $\text{Ps}^*$  with a resonant charge exchange collision,



of trapped  $\text{e}^+$  and Rydberg  $\text{Cs}^*$  atoms. The cross section for such collisions has been calculated [6], but without including the crucial role of the strong magnetic field needed to trap  $\text{e}^+$ . In our demonstration, the

E-mail address: [gabrielse@physics.harvard.edu](mailto:gabrielse@physics.harvard.edu)  
(G. Gabrielse).

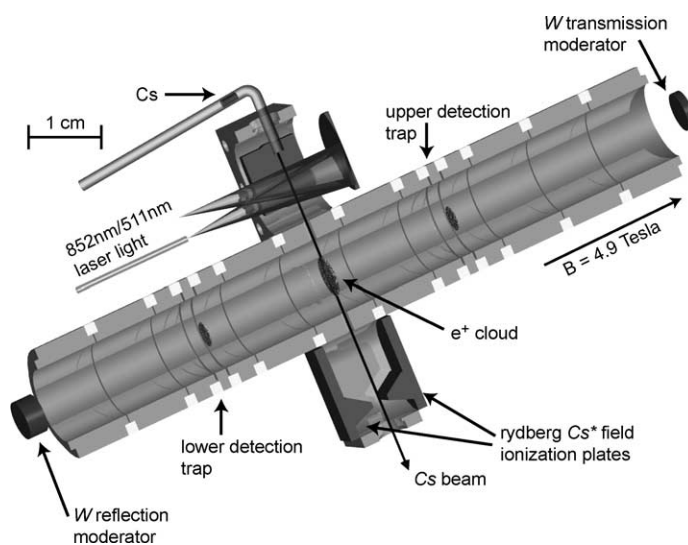


Fig. 1. Trap electrodes, Cs beam and particle locations for producing  $\text{Ps}^*$  via charge exchange collisions of  $\text{Cs}^*$  and trapped  $e^+$ .

$\text{Cs}^*$  is excited from the Cs ground state with infrared diode-laser photons and green copper-vapor-laser photons. The  $\text{Ps}^*$  formed is field ionized; the freed  $e^+$  is captured and then counted. Substantial numbers of  $\text{Ps}^*$  are produced in this demonstration, and a hundred-fold increase should be possible with a larger but manageable radioactive source. Producing antihydrogen by a second charge exchange between the  $\text{Ps}^*$  created in this way and nearby trapped antiprotons ( $\bar{p}$ ) could then be a feasible and important alternative to  $\bar{H}$  production in a nested Penning trap [3] during the  $e^+$  cooling of  $\bar{p}$  [8]—the only method used to produce slow  $\bar{H}$  so far [9–11].

The central part of the apparatus (Figs. 1 and 2(a)) is a series of cylindrical ring electrodes with a 1.2 cm interior diameter, with a strong magnetic field ( $B = 4.9$  tesla) directed along its axis. Voltages applied to the electrodes shape potential wells (Fig. 2(c)) that confine and manipulate trapped particles. Essentially identical electrodes and their 4.2 K vacuum enclosure have been described elsewhere since a very similar apparatus was used to make background-free observations of slow antihydrogen [10] and to probe its internal structure [11]. The elaborate electrode that allows a Cs beam to be sent through the trap differs in its interior only by the addition of two 1 mm holes.

The  $e^+$  accumulation method (described elsewhere [12]) involves slowing  $e^+$  in tungsten crystals, produc-

ing Rydberg positronium, and ionizing this positronium to capture the  $e^+$ . The  $e^+$  originate in a 1 mCi  $^{22}\text{Na}$  source—a strength that can be easily handled in a university laboratory with the appropriate precautions. For this demonstration, time limitations and the condition of our tungsten crystals limited us to accumulating about  $2 \times 10^5 e^+$  for each measurement at a rate of about 4/(s mCi). The  $e^+$  radiate synchrotron radiation to come into thermal equilibrium with their 4.2 K environment. After the  $e^+$  are initially accumulated they are transferred to the  $e^+$  location labeled in Figs. 1 and 2(a).

The number of  $e^+$  is deduced to within a few percent relative accuracy, and to better than 10% absolute accuracy, from the measured width of the notch that they produce in the noise-driven resonance of an attached LCR circuit [13]. The unavoidable length of our electrical leads limits our sensitivity to about  $10 e^+$  here. The density and geometry of  $e^+$  and  $\bar{p}$  plasmas have been previously studied using an aperture method [14]. Based on these studies we estimate that the  $e^+$  plasma is spheroidal (i.e., an ellipsoid with axial symmetry about the  $z$  axis) with an axial extent of 0.8 mm, a diameter of 6.4 mm, and a density of  $1.4 \times 10^7/\text{cm}^3$ .

A Cs beam travels through the trap perpendicular to the magnetic field  $B\hat{z}$  and to the symmetry axis of the trap,  $\hat{z}$ , entering the trap through a 0.3 mm aperture in the first 1 mm hole, mentioned, and leaving the trap through the other 1 mm hole. The Cs comes from

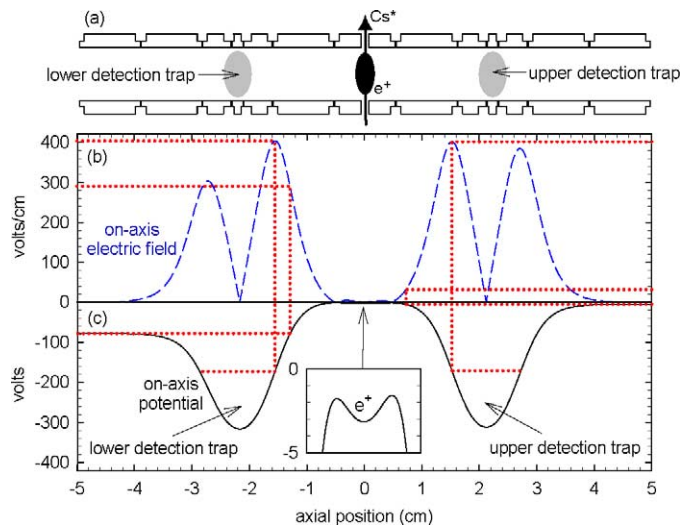


Fig. 2. Cross section of cylindrical ring electrodes (a). Potentials applied to the electrodes produce a potential well that confines  $e^+$  at the center, along with upper and lower detection traps in which  $Ps^*$  are ionized and detected. The on-axis electric field is shown in (b) and the corresponding on-axis potential is in (c). Dotted drop lines identify the minimum and maximum electric fields on the axis within the detection wells.

a small volume ( $\sim 5 \text{ mm}^3$ ) oven when it is heated to about 317 K. Careful thermal isolation of this oven, heat sinking, and thermal shielding made it possible to keep this electrode, originally at 4.2 K, from heating above 5.5 K during the 20 minutes in which heat is typically applied to the oven. About 95% of the ballistic Cs trajectories from the oven that enter the trap through the 0.3 mm aperture leave the trap through the 1 mm hole on the other side of the trap. It is important to avoid Cs deposits on inner electrode surfaces.

Between the oven and the first aperture the Cs atoms are excited from  $6S_{1/2}$  to  $6P_{3/2}$  by approximately 8 mW of infrared 852 nm diode laser light. The light enters the vacuum enclosure for the trap through a 1 mm diameter optical fiber, illuminates Cs atoms traveling toward the trap, reflects from a spherical mirror, and then illuminates the atoms again, so that the two light passes illuminate about 5.8 mm of Cs trajectory. The  $6P_{3/2}$  lifetime is 30 ns and the saturation intensity is  $2.7 \text{ mW/cm}^2$ . We should be saturating this transition despite the frequency modulation used to keep the laser on resonance (avoidable in the future), with a bit more than 35% of the atoms estimated to be excited to  $6P_{3/2}$ . Fluorescence detected with a Si photodiode that views the illumination region simultaneously confirms resonance with the Cs.

To excite the Cs from  $6P_{3/2}$  to a high Rydberg orbit, green light at 511 nm from a copper vapor laser is sent to the Cs using the same fiber and mirror. The 20 ns pulses with a peak power of 750 W repeat every 50  $\mu\text{s}$  to provide an average power of 300 mW—a significant heat load on our cryogenic system. Half of the Cs atoms traveling at the average speed of a 317 K thermal distribution would see a green laser pulse as they traverse the illumination region. The  $37D$  state (lifetime  $\sim 38 \mu\text{s}$ ) would be excited if there was no magnetic field present, but the  $1 \text{ W/cm}^2$  illuminating the Cs is estimated to be far less than needed to saturate the transition. The magnetic field mixes so many different states and principle quantum numbers that the states in the field are difficult to calculate. The number of  $Cs^*$  passing through the trap is thus empirically maximized by tuning the Cs into resonance with our fixed frequency green laser, by varying an electric field that is perpendicular to the Cs path toward the trap and to the light propagation direction.

The number of excited  $Cs^*$  is measured directly by field ionizing them after they exit the trap. Fig. 3 shows the ion current (positive) and the electron current (negative) collected on one of the field ionization plates of Fig. 1 for a high  $\sim 340 \text{ K}$  oven temperature. The current increases when the ionizing electric field magnitude increases above about 100 V/cm and then

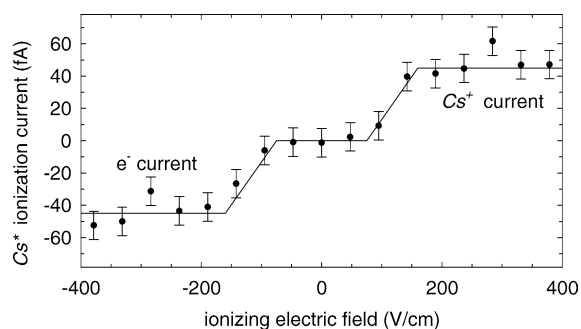


Fig. 3. Current from Rydberg  $\text{Cs}^*$  atoms that field ionize after passing through the trap. The measurements are consistent with (but do not establish) a simple antisymmetric curve that would be expected to describe a current that increases when the electric field becomes strong enough to ionize  $\text{Cs}^*$  atoms and saturates at fields strong enough to ionize all of the  $\text{Cs}^*$ .

saturates. This is consistent with the expected field ionization of  $\text{Cs}^*$  with large radii, and similar to what was observed in tests with no magnetic field and at 0.4 tesla, though the uncertainties are large enough that the curve to aid the eye in Fig. 3 is not determined to a high confidence level. The current changes very little when the infrared laser power is changed, confirming saturation of the  $6P_{3/2}$  state. The current changes in proportion to the intensity of the green laser confirming that the saturation has not been reached for excitation to a highly excited state.

The  $6P_{3/2}$  to  $6S_{1/2}$  fluorescence detected with the photodiode is proportional to the  $\text{Cs}^*$  ionization current. For producing Rydberg  $\text{Ps}^*$ , the oven temperature is reduced to about 317 K to reduce the Rydberg  $\text{Cs}^*$  ionization current by about a factor of 50. This factor is determined from the calibrated  $6P_{3/2}$  fluorescence since the ionization current becomes too small to measure directly. About  $6 \times 10^3$   $\text{Cs}^*/\text{s}$  then pass through the trap.

Excited  $\text{Ps}^*$  is formed when the  $e^-$  from a Rydberg  $\text{Cs}^*$  is captured by a trapped  $e^+$ . The  $\text{Ps}^*$  formed in this resonant charge exchange collision will have approximately the same binding energy as did the Rydberg  $\text{Cs}^*$ —a binding energy determined by the laser frequencies. We detect only excited  $\text{Ps}^*$  atoms that enter the detection wells to either side (Figs. 1 and 2(a)), which have a combined solid angle of only about  $4\pi/32$ . The  $\text{Ps}^*$  entering the detection wells are ionized if the electric field is strong enough. The  $e^+$  from the ionized  $\text{Ps}^*$  is captured if it sees a confining po-

tential at the ionization point. The number of ionized  $\text{Ps}^*$  can thus be counted as were the initially trapped  $e^+$  from the notch that the captured  $e^+$  produce in a noise-driven LCR resonance [13].

Illustrative potentials (solid curve) and electric fields (dashed curve) on the axis of the trap are shown in Fig. 2(b). For a  $e^+$  from an ionized  $\text{Ps}^*$  to be captured in one of the detection wells, an electric field between the minimum and maximum value present in the trap well must ionize the  $\text{Ps}^*$ , as illustrated by the dotted drop lines for  $\text{Ps}^*$  traveling along the trap axis. For example, a  $\text{Ps}^*$  traveling along the trap axis into the upper detection well (right in Fig. 2) will have its  $e^+$  trapped if it ionizes when the field is between 35 and 400 V/cm. The  $e^+$  from a  $\text{Ps}^*$  that ionizes at a field lower than this range will not be trapped. A  $\text{Ps}^*$  that ionizes only at a field higher than this range will not be ionized at all. Similarly, a  $\text{Ps}^*$  traveling along the trap axis into the lower detection well (left in Fig. 2) will have its  $e^+$  trapped only if it ionizes when the field is between 290 and 400 V/cm. These examples illustrate how lowering one side of the potential well with respect to the other changes the minimum ionizing electric field that will deposit a  $e^+$  in a detection well. To ensure that any stray low energy  $e^+$  and contaminant positive ions are not captured, the potential to one side of each of the two detection wells in Fig. 2 is lower than the potential of the opposite side, though one must look closely to see the small offset potential symmetry for the upper detection trap.

The maximum axial ionization field in the detection wells is 400 V/cm or greater—large enough to ionize the  $\text{Ps}^*$  formed by resonant charge exchange. The minimum axial ionization field in the detection wells is varied by changing the asymmetry of the detection wells, to probe the  $\text{Ps}^*$  states that are produced. The electric fields and potentials for all possible  $\text{Ps}^*$  trajectories from the initial positron plasma to the detection wells are important since the potentials and fields are also a function of radial position.

Fig. 4 shows a  $\text{Ps}^*$  field ionization spectrum as a function of the minimum axial electric field within the potential well of the detection trap. The number of detected  $\text{Ps}^*$  does not change as this minimum ionization field is initially increased from zero. The number declines as the minimum field within the detection well is raised further. No  $\text{Ps}^*$  are ionized and detected when the minimum field approaches the max-

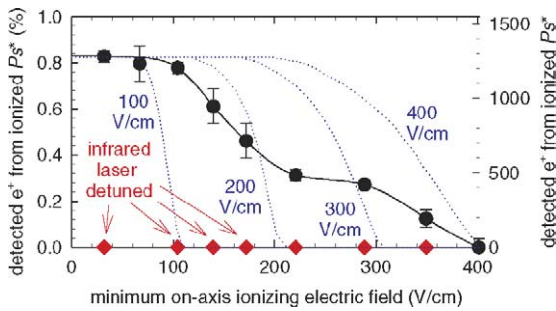


Fig. 4. Detected  $\text{Ps}^*$  as a function of the minimum axial electric field in the detection well. The dotted curves are the spectra obtained by averaging over all possible ballistic  $\text{Ps}^*$  trajectories to the detection traps for  $\text{Ps}^*$  atoms which ionize at the electric fields indicated by the labels.

imum field within the well. When the infrared laser is detuned just off resonance no  $\text{Ps}^*$  is detected (diamonds in Fig. 4), as expected. The dotted lines show calculated spectra expected for  $\text{Ps}^*$  which ionize at the particular ionization fields indicated, averaged over all possible trajectories from the  $e^+$  plasma (6.4 mm in diameter) to the detection well (10 mm in diameter). The spectrum shape indicates that the  $\text{Ps}^*$  ionize for electric fields between 100 and 400 V/cm. The small plateau near 250 V/cm may indicate that there are two separate  $\text{Ps}^*$  populations which ionize at different field strengths. The vertical scale to the right in Fig. 4 gives some idea of the number of  $e^+$  forming  $\text{Ps}^*$  in a typical measurement.

The fraction of trapped  $e^+$  that form Rydberg  $\text{Ps}^*$  and are detected increases with the number of Rydberg  $\text{Cs}^*$  that passes through them to a saturation value of about 0.8%, as shown in Fig. 5. This asymptotic value is about 4 times smaller than what would be expected if all the trapped  $e^+$  formed an isotropic  $\text{Ps}^*$  distribution.

This reduction is possibly related to the number of ground state Cs atoms passing through the trapped  $e^+$  compared to the  $\text{Cs}^*$ , a ratio that we estimate from the measured fluorescence and the  $\text{Cs}^*$  ionization current to be between  $10^3$  and  $10^4$ . Alternatively, it may signal an unexpected, non-isotropic  $\text{Ps}^*$  distribution. The rate for producing ground state Ps [15], which we would not detect, is too small to account for an appreciable fraction of the reduction. It should be possible to check if some of the factor of four is recovered if the relative fraction of  $\text{Cs}^*$  compared to ground state Cs is increased. Currently the infrared laser excites

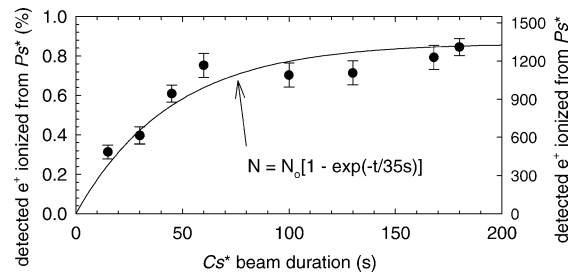


Fig. 5.  $\text{Ps}^*$  production as a function of  $\text{Cs}^*$  beam duration shows a 35 second time constant for 6000 Rydberg  $\text{Cs}^*$  atoms/second. The uncertainties represent average measurement reproducibility. No  $\text{Ps}^*$  is produced and detected when the infrared laser is detuned just off resonance.

only one of the 16 Zeeman hyperfine sublevels of the  $6S_{1/2}$  ground state, for example, so exciting more of these levels with additional infrared lasers could significantly increase the fraction of  $\text{Cs}^*$  passing through the trapped  $e^+$ . Increased green laser power would yield more  $\text{Ps}^*$  but at the expense of increasing the heat load on the cryogenic system.

The number of detected  $\text{Ps}^*$  increases as an exponentially function of the time that the  $\text{Cs}^*$  pass through the trapped  $e^+$ , with a 35 second time constant (Fig. 5). The initial slope in the exponential corresponds to a cross section of  $8(3) \times 10^{-10} \text{ cm}^2$ , which is nearly ten million times bigger than a Bohr cross section. Interestingly, this cross section is not so far from the  $\sigma = 1.5 \times 10^{-9} \text{ cm}^2$  calculated for no magnetic field, despite the fact that the strong field is expected to couple center-of-mass and internal orbits, and make chaotic internal orbits [17].

The strong magnetic field, an essential element of the  $e^+$  trap, complicates this experiment and its theoretical interpretation in several ways. We have already discussed how we empirically vary an electric field to tune a Rydberg  $\text{Cs}^*$  state into resonance with a fixed frequency laser, for example, without knowing which  $\text{Cs}^*$  states we excite because these states have not been calculated. The internal orbits of the Rydberg atoms formed are significantly modified by the field (e.g., [16]) since the magnetic force can be comparable or greater than the Coulomb force, depending upon the size of the atoms. In fact, the binding energies of Rydberg atoms moving across a strong magnetic field are not even conserved, but are instead coupled to the center of mass energy of the atoms [17]. A theory of this charge exchange process done without a magnetic

field [6] gives a guide about what to expect. However, a formation calculation that includes the crucial role of the magnetic field is needed.

This laser-controlled  $\text{Ps}^*$  production mechanism may yield enough  $\text{Ps}^*$  to produce detectable amounts of antihydrogen atoms. With 5 million  $4.2 \text{ K } e^+$  accumulated from a larger radioactive source (as was used for  $\bar{\text{H}}$  measurements [18]), about  $6 \times 10^5$  Rydberg  $\text{Ps}^*$  atoms from an isotropic distribution should be detected in a detection well that is a realizable  $0.5 \text{ cm}$  from the center of the  $e^+$  trap. Filling such a well with  $1 \times 10^6 \bar{p}$  should result in the production about  $250 \bar{\text{H}}^*$  atoms, nearly 50 of which we should detect in a detection well that is centered  $1.3 \text{ cm}$  away from the center of the  $\bar{p}$  well, if the cross section for charge exchange collisions of the  $\text{Ps}^*$  and trapped  $\bar{p}$  is also similar to what was calculated neglecting the strong field that produces chaotic orbits [6]. It should be possible to reliably detect this small number of  $\bar{\text{H}}^*$  using the background free ATRAP field ionization method [10]. Of course, when the Cs beam is on it seems likely that the background pressure will rise above the  $5 \times 10^{-17} \text{ Torr}$  background pressure demonstrated earlier [19]. It must thus be demonstrated that sufficient trapped  $\bar{p}$  survive for  $\bar{\text{H}}$  production.

In conclusion, laser-controlled resonant charge exchange collisions of highly excited  $\text{Cs}^*$  atoms with trapped  $e^+$  produce highly excited  $\text{Ps}^*$  atoms—the binding energy of which is determined by the laser frequencies. With the use of a larger source of  $e^+$ , collisions of the excited  $\text{Ps}^*$  with cold, trapped  $\bar{p}$  should produce detectable amounts of  $\bar{\text{H}}$  whose binding energy is also determined by these laser frequencies. The excited and long lived  $\text{Ps}^*$  should charge exchange efficiently with the trapped  $\bar{p}$ , with a large cross section, because of the large size of the excited  $\text{Ps}$ .  $\bar{\text{H}}$  with the lowest possible center-of-mass energy should be produced (lower than the only such  $\bar{\text{H}}$  energy measured so far [20]) because the less massive  $\text{Ps}^*$  can transfer very little energy to the  $\bar{p}$  as the  $\bar{\text{H}}$  forms.

## Acknowledgements

We are grateful to the CERN, its PS Division and the AD team for delivering the high energy antiprotons. This work was supported by the NSF, AFOSR, the ONR of the US, the German BMBF, and the NSERC, CRC, CFI and OIT of Canada.

## References

- [1] G. Gabrielse, in: P. Bloch, P. Paulopoulos, R. Klapisch (Eds.), *Fundamental Symmetries*, Plenum, New York, 1987, p. 59.
- [2] J.W. Humberston, M. Charlton, F.J. Jacobsen, B.I. Deutch, *J. Phys. B* 20 (1987) L25.
- [3] G. Gabrielse, S.L. Rolston, L. Haarsma, W. Kells, *Phys. Lett. A* 129 (1988) 38.
- [4] M. Charlton, *Phys. Lett. A* 143 (1990) 143.
- [5] C. Wesdorp, F. Robicheaux, L.D. Noordam, *Phys. Rev. Lett.* 84 (2000) 3799.
- [6] E.A. Hessels, D.M. Homan, M.J. Cavagnero, *Phys. Rev. A* 57 (1998) 1668.
- [7] J.P. Merrison, H. Bluhme, J. Chevallier, B.I. Deutch, P. Hvelplund, L.V. Jorgensen, H. Knudsen, M.R. Poulsen, M. Charlton, *Phys. Rev. Lett.* 78 (1997) 2728.
- [8] G. Gabrielse, J. Estrada, J.N. Tan, P. Yesley, N.S. Bowden, P. Oxley, T. Roach, C.H. Storry, M. Wessels, J. Tan, D. Grzonka, W. Oelert, G. Scheppers, T. Sefzick, W. Breunlich, M. Carnegelli, H. Fuhrmann, R. King, R. Ursin, H. Zmeskal, H. Kalinowsky, C. Wesdorp, J. Walz, K.S.E. Eikema, T. Haensch, *Phys. Lett. B* 507 (2001) 1.
- [9] M. Amoretti, et al., *Nature* 419 (2002) 456.
- [10] G. Gabrielse, N.S. Bowden, P. Oxley, A. Speck, C.H. Storry, J.N. Tan, M. Wessels, D. Grzonka, W. Oelert, G. Scheppers, T. Sefzick, J. Walz, H. Pittner, T.W. Hänsch, E.A. Hessels, *Phys. Rev. Lett.* 89 (2002) 213401.
- [11] G. Gabrielse, N.S. Bowden, P. Oxley, A. Speck, C.H. Storry, J.N. Tan, M. Wessels, D. Grzonka, W. Oelert, G. Scheppers, T. Sefzick, J. Walz, H. Pittner, T.W. Hänsch, E.A. Hessels, *Phys. Rev. Lett.* 89 (2002) 233401.
- [12] J. Estrada, T. Roach, J.N. Tan, P. Yesley, G. Gabrielse, *Phys. Rev. Lett.* 84 (2000) 859.
- [13] L.S. Brown, G. Gabrielse, *Rev. Mod. Phys.* 58 (1986) 233.
- [14] P. Oxley, N.S. Bowden, R. Parrott, A. Speck, C. Storry, J.N. Tan, M. Wessels, G. Gabrielse, D. Grzonka, W. Oelert, G. Scheppers, T. Sefzick, J. Walz, H. Pittner, T.W. Hänsch, E.A. Hessels, *Phys. Lett. B* (2004), in press.
- [15] E. Surdutovich, W.E. Kauppila, C.K. Kwan, E.G. Miller, S.P. Parikh, K.A. Price, T.S. Stein, *Nucl. Instrum. Methods B* 221 (2004) 41.
- [16] C.W. Clark, E. Korevaar, M.G. Littman, *Phys. Rev. Lett.* 54 (1985) 320.
- [17] D. Vrinceanu, B.E. Granger, R. Parrott, H.R. Sadeghpour, L. Cederbaum, A. Mody, J. Tan, G. Gabrielse, *Phys. Rev. Lett.* 92 (2004) 133402.
- [18] ATRAP, submitted for publication.
- [19] G. Gabrielse, X. Fei, L.A. Orozco, R.L. Tjoelker, J. Haas, H. Kalinowsky, T.A. Trainor, W. Kells, *Phys. Rev. Lett.* 65 (1990) 1317.
- [20] G. Gabrielse, A. Speck, C.H. Storry, D.L. Sage, N. Guise, D. Grzonka, W. Oelert, G. Scheppers, T. Sefzick, H. Pittner, J. Walz, T.W. Hänsch, D. Comeau, E.A. Hessels, *Phys. Rev. Lett.* (2004), in press.